Phase Transitions and Reversal Mechanisms in Nanosized Magnetic Bars: The Influence of Bulk and Localized Spin Wave Modes

R. E. Camley,^ G. Leaf,* H. Kaper,* M. Yan,* and M. Grimsditch@

^ Physics Department, University of Colorado, Colorado Springs, CO 80918

*Mathematics and Computer Science Division, Argonne National Laboratory, Argonne, IL 60439

@ Materials Science Division, Argonne National Laboratory, Argonne, IL 60439

Abstract

Changes in symmetry of the magnetic groundstate of a Co bar as a function of an external field are found to be concomitant with soft spin excitations. The symmetry of the soft modes is found to predict the change in symmetry of the ground state, providing strong evidence that the soft modes are responsible for all the magnetic phase transitions observed in this system. Results are presented in which the Co bar reaches domain states with 3, 5, 12, and 13 domains. None of these states corresponds to the minimum energy state with six domains.

Introduction

Stripe domains appear in many different physical systems and are known to arise from an interplay between short-range forces, atomic bonding or magnetic exchange, and long-range forces, which can be due to electric or magnetic dipolar forces or to elastic strains. Landau and Lifshitz [1] were the first to propose a formalism that describes the energetics of stripe domain formation. In this formalism, where the energy is expanded in terms of an "order parameter" (e.g., magnetization or polarization for ferromagnets and ferroelectrics, respectively), it is easy to see that the formation of stripe domains can lead to a reduction of the total energy of the system. Identifying the order parameter is not easy, however, and it is unclear how a particular system evolves into a stripe domain pattern with long range order.

In this paper we study the influence of dynamics in the magnetic system on the formation of stripe domains. Recently, spin-wave excitations in different magnetic structures have been studied extensively. For example, spin-wave modes in rectangular elements with field dependence were studied by several groups [2-4]. In some dynamical studies, soft modes with frequencies approaching zero were reported at phase transition points [5-9], some of which are believed to be related to the nucleation of domain structures.

We recently investigated a magnetic system, a nanosized Co bar with competing uniaxial anisotropy and shape anisotropy that exhibits stripe domains. In that paper [8] we showed that it was not energy minimization but the magnetic history of the bar that determined the domain pattern at remanence. Furthermore, we studied a particular process where the bar was initially magnetized along the long axis and then the field was reduced. In this case the domain pattern at remanence could be directly connected to a particular spin excitation, a bulklike standing-wave mode, which went soft near the transition to the stripe domain state.

In this paper we examine the more general relationship between soft spin modes (modes whose frequencies approach zero) and the onset of magnetization reversal or other changes in the magnetic spin configuration. We show that changes in the symmetry of the magnetic ground state are always closely associated with soft spin modes and that these modes may be either localized as in the case of end modes or edge modes or extended as in the case of standing spin waves. Furthermore in some cases, the nature of a particular reversal pattern or phase transition may be understood from the behavior of the magnetic excitations at external magnetic fields far away from a critical field.

Physical System and Simulation Details

In this manuscript we calculate the magnetization reversal behavior, both static and dynamic, for different directions of a field applied to a single crystal *hcp* Co bar with in-plane uniaxial anisotropy. The Co bar is 800nm in length, 120 nm in width, and 40 nm in thickness, almost identical to that investigated in [8]. The long and short edges are aligned perpendicular to the c-axis to allow the shape anisotropy to compete with a uniaxial magnetocrystalline anisotropy.

We calculate the complete spectrum of normal-mode spin excitations by diagonalizing a dynamical matrix for small oscillations [10]. The ground-state configuration, for any given external field is obtained by using the OOMMF micromagnetics code [11]; then, the small amplitude, oscillation frequencies are calculated by using the dynamical matrix approach. In the discretization for the dynamical matrix, we use a unit cell that is 20 nm x 20 nm x 40 nm, where the long axis is along the thickness of the Co bar, and we use the Newell tensor approach [12] to obtain the self- and interaction dipole terms for these noncubic cells. The 240 cells in our particle result in 240 normal modes. The input material parameters for both the OOMMF micromagnetic simulations and the normal-mode calculations are the saturation magnetization M_s=1.4 x 10^5

A/m, the exchange constant A = 3 x 10^{-11} J/m and the uniaxial anisotropy constant K_u= 5.2 x 10^5 J/m^3; all are typical values for epitaxial cobalt films.

We note that the results of this method compare very well [13] with a scheme that involves calculating the time evolution of the system and performing a Fourier transform to obtain the frequency response [8].

Results

Here we investigate the relationship between soft magnetic normal modes and the evolution of the symmetry of the ground state during magnetization reversal. To do so we explore four different reversal processes, each of which leads to a different intermediate and final state. The four processes and their key outcomes are described below. The relevant magnetic groundstates encountered at remanence in each case, are illustrated in Fig. 1.

1) A large field is applied along the long axis of the bar. As the field is reduced to zero, the bar breaks up into 12 or 13 stripe domains (Fig. 1a) depending on subtle details that will be described. Both a bulk and a localized phase transition occur during this process. We will show that each phase transition is associated with a softening of a particular spin excitation that has the symmetry of the final state. In particular, as was shown in [8], the symmetry of the remanent stripe domain state is due to a soft, bulklike, standing spin wave mode.
2) A large field is applied along the short axis of the bar. As this field is reduced and then made negative, the bar breaks up into five domains (Fig. 1b). Although at the critical field the magnetization appears to discontinuous, indicating a first order transition, we do find a soft mode with a symmetry consistent with a five-domain structure.

3) Using the same field history as in case (2) above but with an initial state that has a left-right asymmetry in its magnetic configuration, we find an asymmetric three-domain state (Fig. 1c) where reversal is nucleated on one side of the bar only. A soft mode is also found in this case.
4) A large field is applied at a small angle to the short axis of the bar. As this field is reduced and then made negative, the bar breaks up into a symmetric three-domain pattern (fig. 1d). Again, this appears to be a first order transition, but in the dynamics we find a number of modes that approach zero frequency.

Case 1

We first consider the geometry with the applied field along the long axis of the bar. The conclusion that in this case the final stripe domain configuration is due to a soft bulk spin excitation was presented in [8]. Here we focus more on the precursor endlike transitions and the subtle issues that can lead to the formation of 12 or 13 domains. The magnetic configuration for different fields is illustrated in Fig. 2. The high-field state is shown in Fig. 2a. This state is known as a "flower" state because of the spreading out of the magnetic moments and the end of the bar. This state is symmetric about a horizontal line in the middle of the film, and this symmetry will play a key role in what follows. As the field is reduced, two possibilities arise:

1) If there is a small component of the external field upward (i.e., the field is applied at a small angle to the long axis of the bar), then near H= 7.2 kOe there is an effective phase transition that is nucleated at the ends of the bar. At this point, the net magnetic moment at both ends of the bar points upward, and this structure becomes "frozen-in" as the field is reduced. This structure is illustrated in Fig. 2b. Eventually one finds a stripe-domain structure with 13 domains, which is shown in Fig 2c [13].

2) If the external field has no symmetry-breaking component (i.e., it is applied *exactly* along the long axis), then small numerical fluctuations eventually break the symmetry of the structure. Under these conditions we sometimes find a state where the net magnetic moment at one end of the bar points upwards and the net moment at the other end of the bar points downwards. This transition occurs near H = 6.4 kOe and is illustrated in Fig. 2d. In this case the structure at remanence has 12 domains and is illustrated in Fig. 2e.

The frequencies of the normal modes at each field can give us additional insight into the nature of the phase transition. These modes can be roughly classified as localized modes, which include end modes, corner modes, and edge modes, and bulk modes, which resemble standing-wavelike solutions. When the frequencies of two modes are almost equal, hybridization between them can blur this classification scheme.

In Fig. 3 we have plotted the frequency of some of the normal modes as a function of field for the case where the magnetic field is applied at a small angle, .057°, with respect to the long axis. We have chosen to plot only the lowest-frequency bulk mode -- shown by the full line, the lowest-frequency localized modes (labeled "end modes") and a few of the other lower-frequency endlike modes (labeled localized modes). At high fields many localized modes have frequencies that lie below the lowest-frequency bulk mode. As the external field is reduced, however, the bulk mode becomes the lowest-frequency mode in the particle; and, when the frequency of the bulk mode reaches zero just below 5 kOe, the sample nucleates the stripe domain pattern that is observed at remanence. This phase transition has been discussed in detail in Ref. [8] and will not be repeated here. Instead we will concentrate on the end-modes that, if we extrapolate their high field values, would indicate a transition at around

6 kOe. The mode profiles for the two lowest-frequency end modes at H = 8 kOe are shown in Fig. 3b-c, respectively. The profile is an instantaneous snapshot of the component of magnetization perpendicular to the surface. White indicates a moment pointing up and black indicates a moment pointing down. Grey indicates a small amplitude motion or a motion with no vertical component. These modes are labeled symmetric (S) and antisymmetric (AS) end modes [3, 14]; they are almost degenerate with frequencies at 4.679 and 4.677 GHz, respectively.

As discussed above, the slight asymmetry in the direction of the applied field leads to a "preemptive" phase transition at around 7.2 kOe where the net magnetic moment at each end of the bar increases rapidly (Fig 2b). The importance of the alignment of the field has also been emphasized in Ref. [9]. This causes the frequencies of the lowest end modes to increase. Strictly speaking, this is not a phase transition: the symmetry of the magnetic structure has not changed. For fields above 7.2 there is already a small net moment at the ends of the bar that points up because of the external field. Below 7.2 kOe, however, this net moment increases rapidly and quickly reaches its maximum value. Thus one has an “almost” phase transition with an order parameter that is very small (but not zero) before the phase transition and which rises rapidly after the transition. The differences in the structure before and after this phase transition can be seen by comparing Fig. 2a and Fig. 2b. Note that the visual change in magnetization has the same symmetry as the symmetric end mode shown in Fig. 3b.

Below 7 kOe the soft bulk mode decreases in frequency faster than any of the end modes, and it is the bulk mode that first reaches zero frequency just below 5 kOe. As we have shown earlier [8], the wavelength of this mode matches the domain pattern found at remanence. Thus in this geometry, the remnant state configuration is directly connected with a particular bulk mode that is driven to zero frequency.

Figure 4 shows the frequency of the normal modes for the case where the applied magnetic field lies *exactly* along the long axis of the bar. The key difference between Fig. 3a and Fig. 4 is in the behavior of the lowest frequency end modes. Because there is no symmetry-breaking component to the magnetic field for the Fig. 4 case, the flower state remains stable over a wider range of magnetic fields. As a result, the frequency of the lowest end modes continue to decrease as the magnetic field decreases below 7 kOe. In this case a "real" phase transition occurs when an end mode frequency is driven to zero, at around 6.3 kOe. Because the S and AS end modes (see Fig. 3b and c) essentially degenerate, the behavior below 6.3 kOe will depend on which one of the two becomes unstable first. If it is the S end mode, the behavior is identical to that described in Fig. 3. If it is the AS end mode, the particle develops the symmetry shown in Fig. 2d. In this case the bulk phase transition to a stripe domain remanent state still occurs just below 5 kOe, but here the wavevector of the soft mode leads to the formation of the 11-domain stripe structure shown in Fig. 2e.

Cases 2 and 3

For these two cases the bar is initially saturated by a large field along the easy axis (the y direction, perpendicular to the length of the bar). The field is reduced and then made negative. The two cases differ only in the symmetry of the initial state used in OOMMF to calculate the groundstate at each field. Case 2 is conceptually simpler since the initial state at large fields is chosen to be the fully saturated state (all spins aligned along y). In this case the resulting groundstate at all fields above the reversal field maintains the particle symmetry. However, because this 'perfect symmetry' leads to complexities in the dynamics, we relegate its discussion to the appendix.

For case 3 the complications are circumvented by choosing an initial magnetic configuration that does not have left-right symmetry. (We

stress: this is not the same as choosing a groundstate with broken left-right symmetry. The groundstate is still obtained using the OOMMF code. The differences between the two cases reflect the fact that the groundstates generated by OOMMF depend on subtle changes in the initial magnetization profile). For fields above -2.25 kOe the resulting groundstate is indistinguishable from the one obtained using a symmetric initial configuration and is shown in Fig. 6a. For fields below -2.25 kOe however, the resulting groundstate does not have left-right symmetry as shown in Fig. 6b.

The frequencies of the lowest modes for case 3 are shown in Fig. 5. The arrows indicate two soft (or nearly soft) modes and each of these softenings occurs concomitantly with a change in the symmetry of the magnetic structure of the bar. Near H_y = -2.25 the nearly soft mode in Fig. 5 indicates that this structure is unstable resulting in the center of the flower moving away from the center of the bar, either to the right or left as illustrated in Fig. 6b. This change in groundstate stabilizes the soft-mode and its frequency then rises as the field is further reduced. Near H_y = -2.42, however, a second mode goes soft very rapidly and leads to the onset of the formation of a reversed domain as we shall see below.

The spatial profiles of the soft eigenmodes give additional information about the nature of the phase transitions. In Fig. 6c we show the out of plane component of the precessing magnetization for the softest mode at -2.25 kOe. For this mode the spin motion along the top edge of the bar is 180° out of phase with that of the motion at the bottom edge. This means, for example, that when the spins at the top are tilted to the left, the ones at the bottom are tilted to the right. When this mode goes soft, one might expect to add these deviations to the old equilibrium state in order to find the new stable configuration. Such a process produces a state where the center of the flower is shifted to the right as shown in Fig. 6b. Thus the nature of this first transition, the shift in the center position of the flower, is directly connected to a particular soft

mode found in the dynamics. In fact, since the mode pattern of this low frequency spin wave remains nearly unchanged in character for fields above H_y = - 2.25, its behavior at fields well above the actual transition can be used to predict the nature of the oncoming phase transition.

Figure 7a shows the eigenmode profile for the rapidly decreasing eigenmode at H_y = -2.432 kOe. Note that this mode has a large amplitude in the region away from the center of the flower state (Fig. 6b). Figure 7b shows the spin configuration during the initial stages of the reversal process at -4.44 kOe as calculated by OOMMF. We stress that this *is not* an equilibrium configuration and represents only an instantaneous snapshot during the reversal. Clearly, reversal starts at a distance of about 250 nm from the end of the bar, and that this precisely matches the position where the spin motion has its largest amplitude. Once equilibrium is reached the configuration in Fig. 7b has changed to that shown in Fig. 1c.

Case 4

In the final example, the magnetic field is directed at a small angle, 2.87°, with respect to the easy anisotropy axis. Again the field is initially large and saturates the sample. When the field is reduced and made negative, a phase transition occurs near H_y = -2.1 kOe. In Fig. 8 we plot the frequencies of the lowest few modes as a function of external field. One clearly sees several modes becoming soft near H_y = -2.1 kOe. Although the physical situation is very similar to the previous example, however, one finds a very different reversed state; compare Figs. 1c and 1d. The spatial profile of the softest mode in Fig. 8 is shown in Fig. 9a. Figure 9b is the magnetic configuration (not a stable state) obtained with OOMMF just after the onset of the phase transition. Again these two calculations give complementary results, and near H_y = -2.1 kOe the central portion of the bar reverses creating a three-domain state (Fig. 1d).

Conclusions

From micromagnetic simulations and normal mode calculations, we have studied the connection between soft eigenmodes and phase transitions during magnetization reversal in a Co bar. Micromagnetic simulations were performed by using the OOMMF code. Normal modes were calculated by using a dynamical matrix approach. For a number of field directions and field histories we find that all changes in the symmetry of the magnetic groundstate are concomitant with a soft eigenmode. The symmetry of the soft mode is found to correlate with the change in the symmetry of the groundstate. In the case of our Co bar all except one of the phase transitions involve eigenmodes that are dominated by surface effects. The transition involving a bulk eigenmode, as reported in [8], leads to the well-known stripe domain pattern at remanence.

Acknowledgements

The work of G.L., H.K., and M.Y. was supported by the Mathematical, Information, and Computational Sciences Division, Advanced Scientific Computing Research program, and M.G. was supported by the Basic Energy Sciences/Materials Sciences program, both programs under the Office of Science, U.S. Dept. of Energy, under Contract No. W-31-109-Eng-38. R. C. thanks the Argonne Theory Institute for support during his stay at ANL, and that work was also supported by DOA Grant No. W911NF-04-1-0247.

Appendix: Case 2

We return here to the results for case 2 that, as mentioned in the main text, contain some subtle complications. We include it because it is one of the most "obvious" cases to treat and its omission would therefore

be misleading. We have seen in case 3 that, starting from a positive vertical field, when the external field is made sufficiently negative, a phase transition occurs in which the center of the flower state moves toward one side of the magnetic bar. In contrast, if left-right symmetry is not intentionally broken, the centered flower state remains stable (within OOMMF) until a field near H_y = -2.5 kOe. At this field the bar breaks up into five domains, as seen in Fig. 1b. Because this transition shows a dramatic change in magnetization as a function of field it could represent a first order transition in which a soft mode is not required. Nonetheless, we find a distinct signature of a nearly soft mode in the excitation spectrum. In Fig A1 we present the frequencies of the lowest few modes found by using the dynamical matrix method. If one ignores for now the mode that goes soft just above -2.4kOe, just below H_y = -2.5 there is a dramatic softening of several modes; if these modes were the soft modes responsible for the transition they would yield a transition at a field in good agreement with the OOMMF calculations. Even more compelling is that Fig. A-2a, which shows the out of plane component of the precessing magnetization of the lowest mode at -2.5 kOe, has the correct symmetry and profile to explain the transient OOMMF configuration at the onset of the transition shown in Fig. A-2b. Both indicate that reversal starts at a distance of 200nm from the ends of the bar.

The complicating factor in this analysis, however, is the fact that another mode goes soft at a higher field, near H_y = -2.4 kOe. Unlike all the examples in the main text, however, where in every groundstate we always found 240 real eigenfrequencies, in this case, below -2.4 kOe, we find only 239 real eigenfrequencies and one imaginary one. This finding should indicate that the magnetic structure (in the dynamical calculation) is unstable below H_y = -2.4 kOe and that the resulting dynamics of the system may, or should not, be correct. This belies however, the good agreement described in the previous paragraph

between the OOMMF reversal path and the profile of the second soft mode.

There are two possible explanations for this behavior:

1) There may be slight differences between the energies (and or numerical accuracies) used to derive the effective fields in OOMMF and in our dynamical calculations. With this explanation both methods are "correct within their framework" and differ only in that the centered flower state is stable in one formalism and unstable in the other. It follows that if the identical effective fields could be used for the dynamics, the lowest mode at H_y = -2.4 kOe (see profile in Fig. 7a) would not be the first to go soft. The reversal behavior would then be as shown in Fig. A2, leading to the five-domain state in Fig. 1b. We attempted to check this explanation by varying the material parameters in the dynamical calculations: we were unable to change the ordering of the soft mode frequencies.
2) The second explanation is that the centered flower state, although not strictly stable, is numerically stable within OOMMF because of its high symmetry. We attempted to check this explanation by using a state in OOMMF where a spin in one of the corners of the bar was removed. In that case the centered flower state becomes unstable at a field of about -2.1 kOe and shows a distinct shift toward the side of the bar with the removed spin. The transition to the reversed domain structure then proceeds similarly to that found in Fig. 7, with the reversal occurring only on one side of the bar.

Although the origin of this stability/instability obviously requires further attention, it is essentially only a problem of theoretical interest. In all experiments perfect symmetry will be broken either by imperfect alignment of the applied field or by imperfect shapes of the particle.

Conceptually however understanding this issue poses an interesting challenge.

References

1 L. Landau and E. Lifshitz, Phys. Zs. Sow. **8**, 153 (1935) and *Electrodynamics of Continuous Media*, Pergamon, Oxford (1960)

2 G. Gubbiotti, M. Conti, G. Carlotti, P. Candeloro, E. D. Fabrizio, K. Y. Guslienko, A. Andre, C. Bayer, and A. N. Slavin, J. Phys: Cond. Matt. **16**, 7709 (2004).

3 M. Grimsditch, G. K. Leaf, H. G. Kaper, D. A. Karpeev, and R. E. Camley, Phys. Rev. B **69**, 174428 (2004).

4 C. Bayer, J. Jorzick, B. Hillebrands, S. O. Demokritov, R. Kouba, R. Bozinoski, A. N. Slavin, K. Y. Guslienko, D. V. Berkov, N. L. Gorn, and M. P. Kostylev, Phys. Rev. B **72**, 064427 (2005).

5 R. D. McMichael, M. J. Donahue, D. G. Porter, and Jason Eicke, *J. Appl. Phys.* **89**, 7603 (2001).

6 Matthieu Bailleul, Dominik Olligs, and Claude Fermon, *Phys. Rev. Lett.* **91**, 137204 (2003).

7 M. Yan, H. Wang, P. A. Crowell, and C. E. Campbell, *Condensed Matter Theory* **20**, 251, NOVA SCIENCE PUBLISHERS, INC (2005).

8 G. Leaf, H. Kaper, M. Yan, V. Novosad, P. Vavassori, R. E. Camley, and M. Grimsditch, Phys. Rev. Lett. **96**, 017201 (2006).

9 B. B. Maranville, R. D. McMichael, S. A. Kim, W. L. Johnson, C. A. Ross and Joy Y. Cheng, J. Appl. Phys. **99**, 08C703 (2006).

10 M. Grimsditch, L. Giovannini, F. Montoncello, F. Nizzoli, G. Leaf and H. Kaper, Phys. Rev. B **70**, 054409 (2004).

11 J. Donahue and D. G. Porter, *OOMMF User's Guide, Version 1.2 alpha 3* (National Institute of Standards and Technology, Gaithersburg, MD, 2002).

12 A. J. Newell, J. Geophys. Res. **98**, 9551 (1993).

13 We note that the precise number of domains (13) found at remanence in this manuscript is slightly different from that found earlier (11) for a similar structure [8]. This is a result of the

different discretizations and computational techniques used in the two papers. This paper uses a larger cell size because of the computation demands of the normal mode dynamics via the dynamical matrix method. Although the number of domains is slightly different in the two papers, we stress that the physics of the situation including the soft-mode behavior is fundamentally reproduced by the dynamical matrix approach.

14 R. D. McMichael and M. D. Stiles, J. Appl. Phys. **97**, 10J901 (2005)

Figure Captions

Figure 1: Sample equilibrium configurations found by using OOMMF after different field histories. In (a) a large field is applied along the long axis of the bar and then reduced to zero. In (b) a large field is applied along the short axis of the bar. As this field is reduced and then made negative, the bar breaks up into five domains. Configuration (c) uses the same field history as in (b) but with an initial state that is slightly modified to introduce some left-right asymmetry in the magnetic configuration. In (d) a large field is applied at an angle to the short axis of the bar. As this field is reduced and then made negative, the bar breaks up into three domains.

Figure 2: Equilibrium configurations at various fields found using OOMMF after different field histories: (a) flower state when the external field is applied along the long axis of the bar; (b) symmetric end state when a large field is applied at a slight angle to the long axis and then reduced to 7 kOe; (c) final configuration when the field is reduced from 7 kOe to 0; (d) asymmetric end state occuring when a large field is applied exactly along the long axis and then reduced to 4.82 kOe; (e) final state when the configuration in (d) has the field reduced to zero.

Figure 3: a) Eigenmode frequencies found when a field is applied at an angle of .057°with respect to the long axis of the bar; b) profile of symmetric end mode; c) profile of antisymmetric end mode. The profile is an instantaneous snapshot of the component of magnetization perpendicular to the surface. White indicates a moment pointing up and black indicates a moment pointing down.

Figure 4: Eigenmode frequencies found when a magnetic field is applied exactly along the long axis of the bar.

Figure 5: Eigenmode frequencies found when the magnetic field is applied along the easy (short) axis of the bar. The field starts at a large positive value and is then reversed and made negative.

Figure 6: Spin configurations found at different fields for the case where a large external field is initially in the y direction and then is reversed. Note that in (b) the center of the flower has shifted to the right. Shown in (c) is a snapshot of the out-of-plane component of the precessing magnetization for the lowest eigenmode in Fig 5 at H_y = -2.25 kOe.

Figure 7: (a) Out-of-plane component for the eigenmode in Fig. 5 with the rapid decrease at H_y = -2.432 kOe; (b) transient spin configuration found by micromagnetic simulations at H_y = -2.44 kOe.

Figure 8: Frequency versus magnetic field for the lowest frequency modes when a large magnetic field is applied at a 2.87° with respect to the anisotropy axis and then reduced and made negative.

Figure 9: (a) Out-of-plane component for the eigenmode in Fig 8 with the rapid decrease at H_y = -2.16 kOe and 3.37 GHz, where white is 0 and black is 1; (b) Transient spin configuration found by micromagnetic simulations at H_y = -2.2 kOe.

Figure A-1: Frequency versus magnetic field for the lowest frequency modes when a large magnetic field is applied along the anisotropy axis and then reduced and made negative. The equilibrium state is always the centered flower state.

Figure A-2: (a) Out-of-plane component for the 2.731 GHz eigenmode in Fig 8 with the rapid decrease at H_y = -2.503; (b) transient spin configuration found by micromagnetic simulations at H_y = -2.51 kOe.

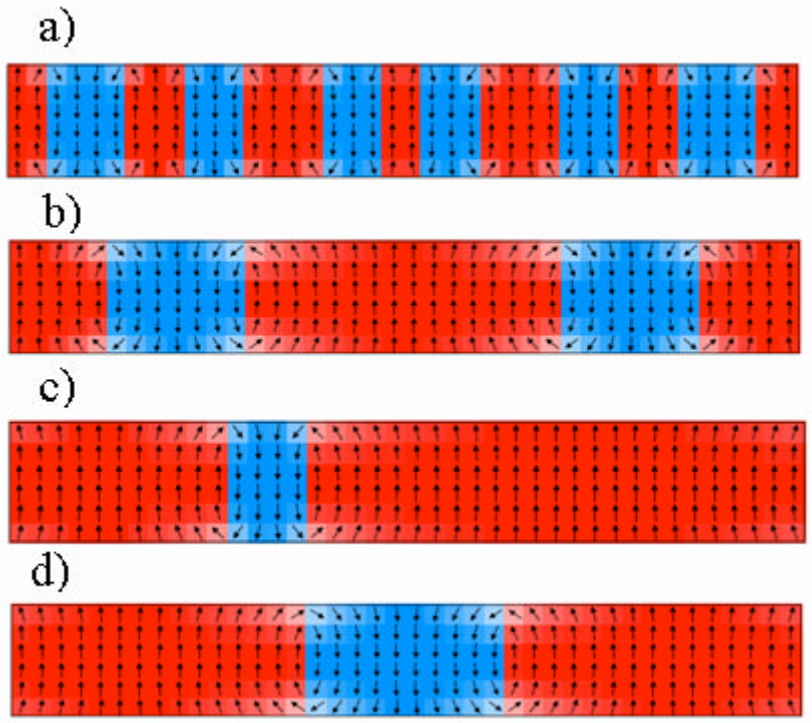

Figure 1: Sample equilibrium configurations found by using OOMMF after different field histories. In (a) a large field is applied along the long axis of the bar and then reduced to zero. In (b) a large field is applied along the short axis of the bar. As this field is reduced and then made negative, the bar breaks up into five domains. Configuration (c) uses the same field history as in (b) but with an initial state that is slightly modified to introduce some left-right asymmetry in the magnetic configuration. In (d) a large field is applied at an angle to the short axis of the bar. As this field is reduced and then made negative, the bar breaks up into three domains.

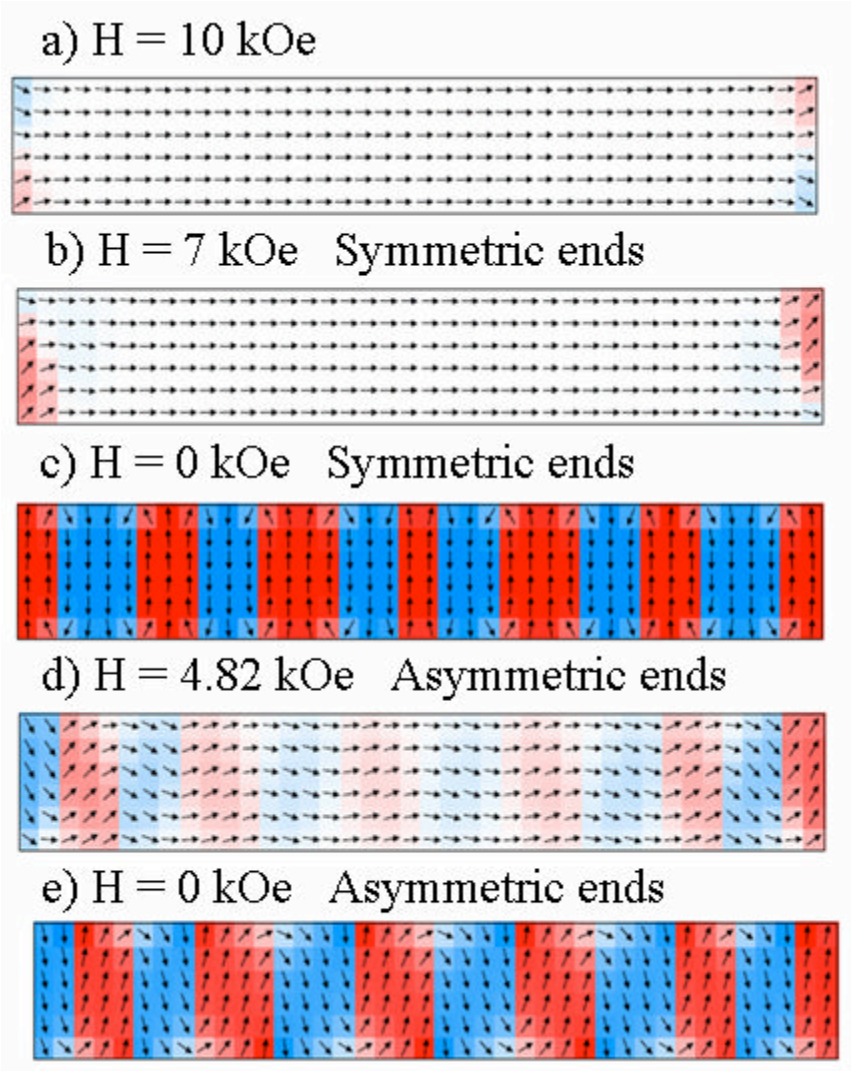

Figure 2: Equilibrium configurations at various fields found by using OOMMF after different field histories: (a) flower state when the external field is applied along the long axis of the bar; (b) symmetric end state when a large field is applied at a slight angle to the long axis and then reduced to 7 kOe; (c) final configuration when the field is reduced from 7 kOe to 0; (d) asymmetric end state occuring when a large field is applied exactly along the long axis and then reduced to 4.82 kOe; (e) final state when the configuration in (d) has the field reduced to zero.

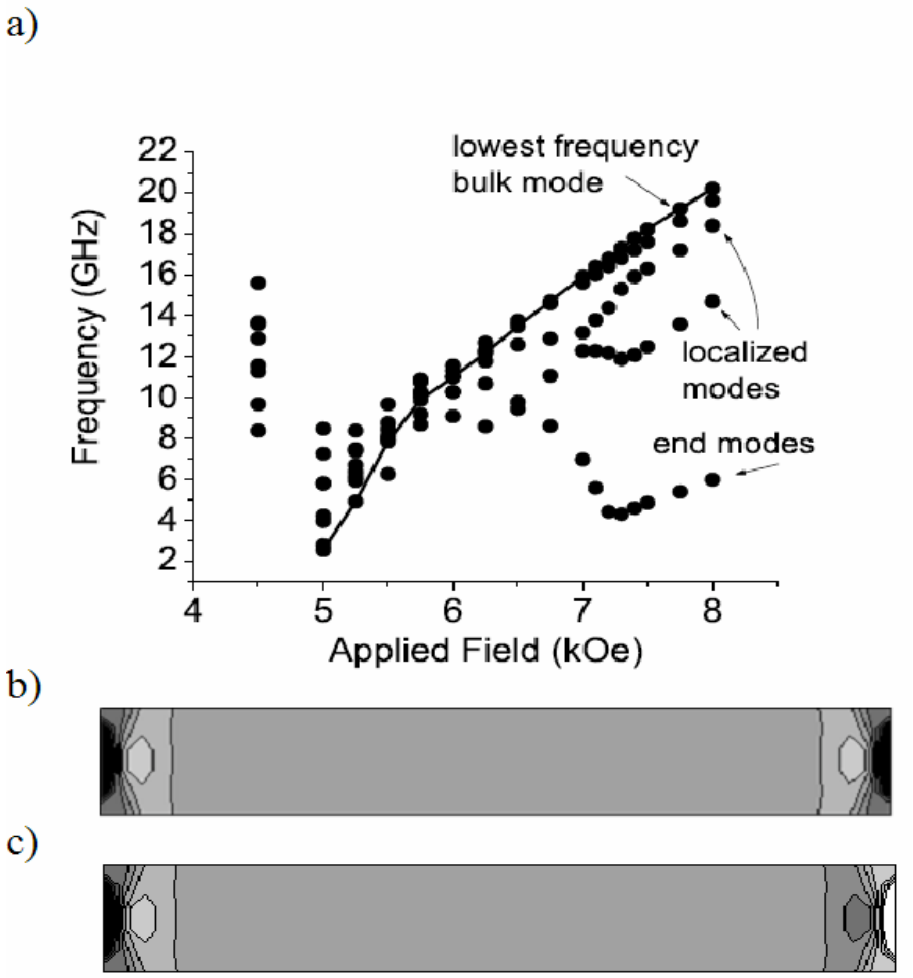

Figure 3: a) Eigenmode frequencies found when a field is applied at an angle of .057°with respect to the long axis of the bar; b) profile of symmetric end mode; c) profile of antisymmetric end mode. The profile is an instantaneous snapshot of the component of magnetization perpendicular to the surface. White indicates a moment pointing up and black indicates a moment pointing down.

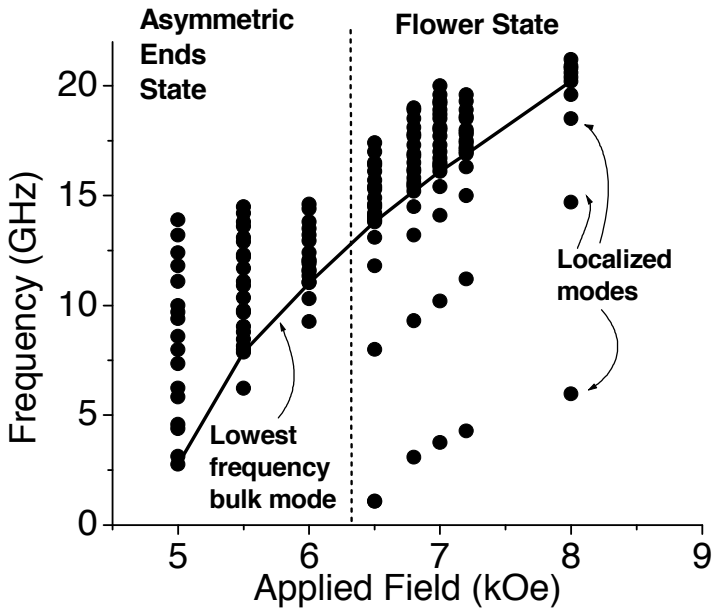

Figure 4: Eigenmode frequencies found when a magnetic field is applied exactly along the long axis of the bar.

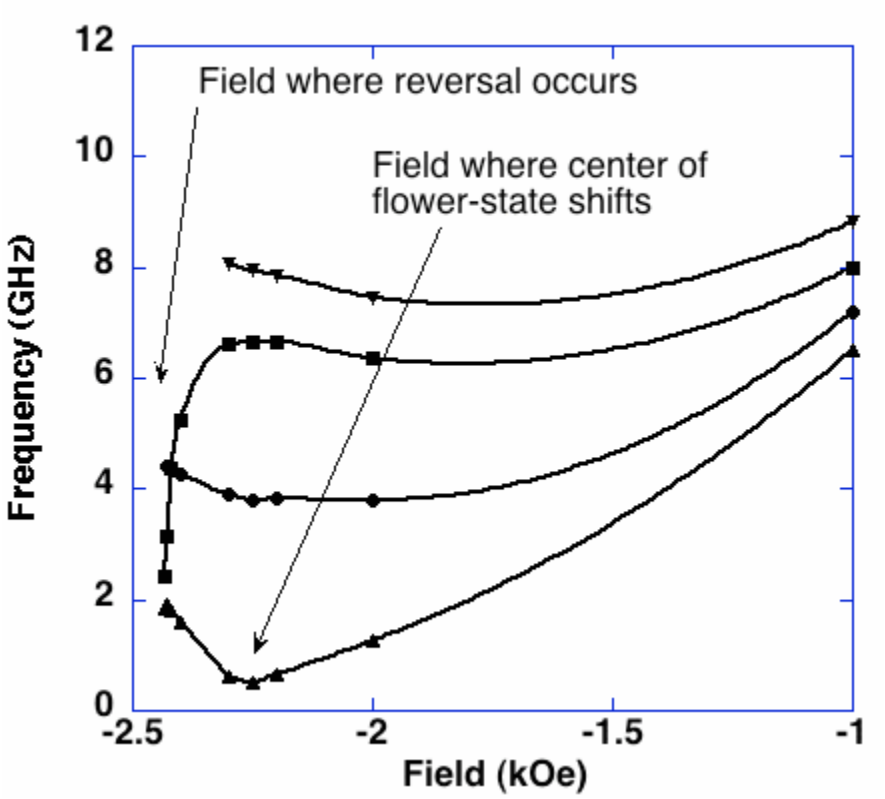

Figure 5: Eigenmode frequencies found when the magnetic field is applied along the easy (short) axis of the bar. The field starts at a large positive value and is then reversed and made negative.

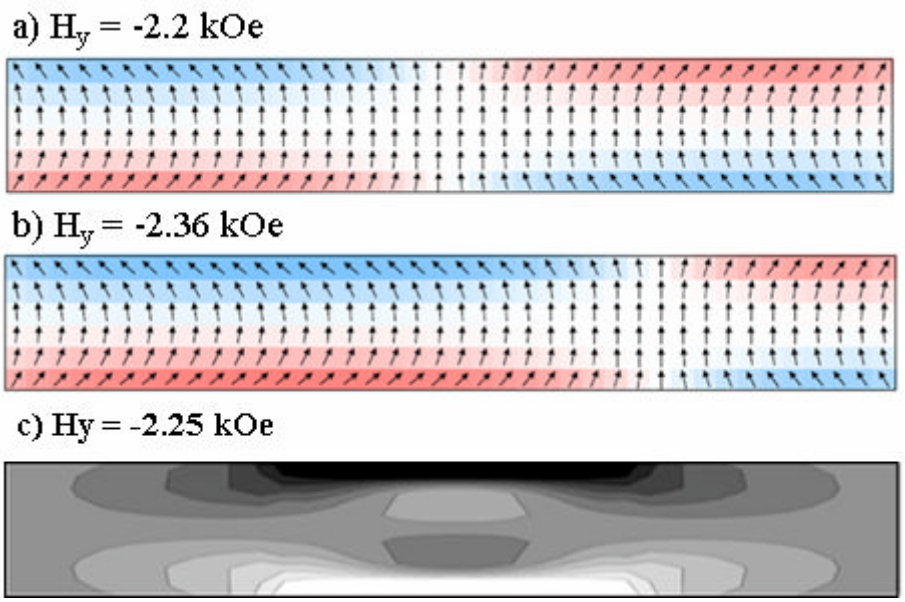

Figure 6: Spin configurations found at different fields for the case where a large external field is initially in the y direction and then is reversed. Note that in (b) the center of the flower has shifted to the right. Shown in (c) is a snapshot of the out-of-plane component of the precessing magnetization for the lowest eigenmode in Fig 5 at H_y = -2.25 kOe.

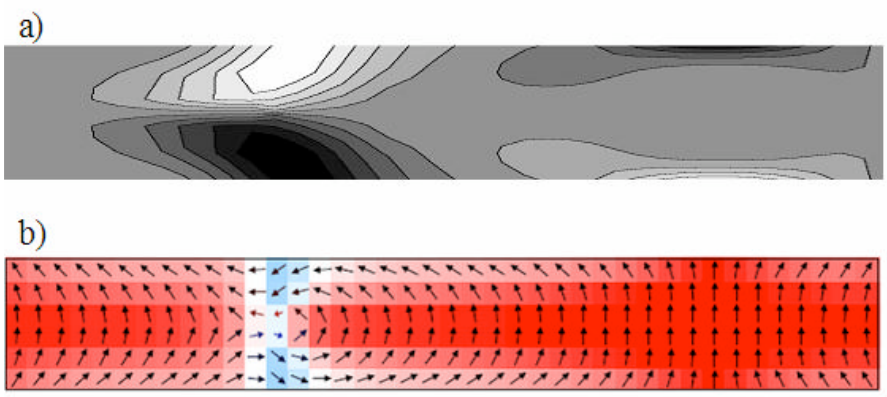

Figure 7: (a) Out-of-plane component for the eigenmode in Fig 5 with the rapid decrease at H_y = -2.432 kOe. (b) Transient spin configuration found by micromagnetic simulations at H_y = -2.44 kOe.

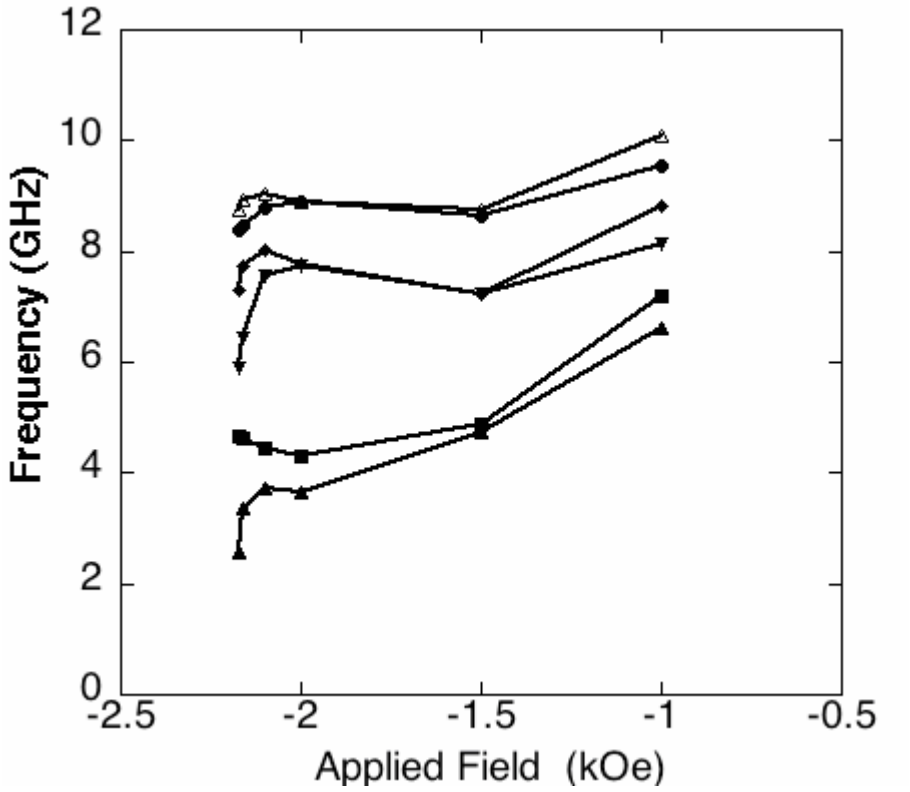

Figure 8: Frequency versus magnetic field for the lowest-frequency modes when a large magnetic field is applied at a 2.87° with respect to the anisotropy axis and then reduced and made negative.

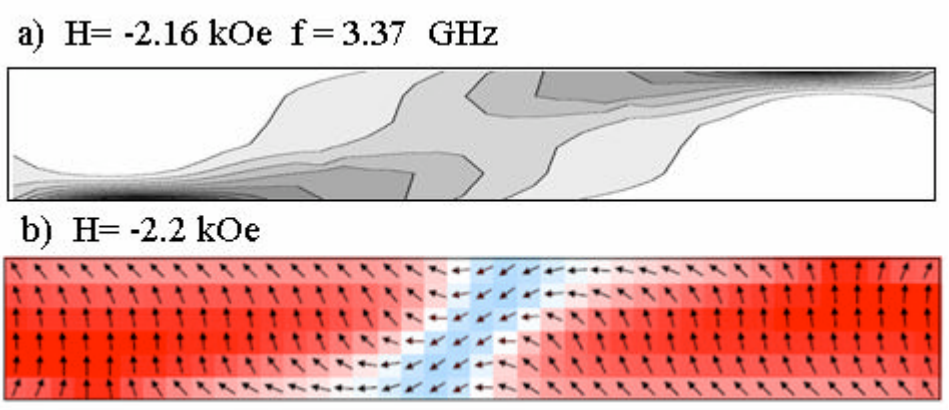

Figure 9: (a) Out-of-plane component for the eigenmode in Fig 8 with the rapid decrease at H_y = -2.16 kOe and 3.37 GHz, where white is 0 and black is 1. (b) Transient spin configuration found by micromagnetic simulations at H_y = -2.2 kOe.

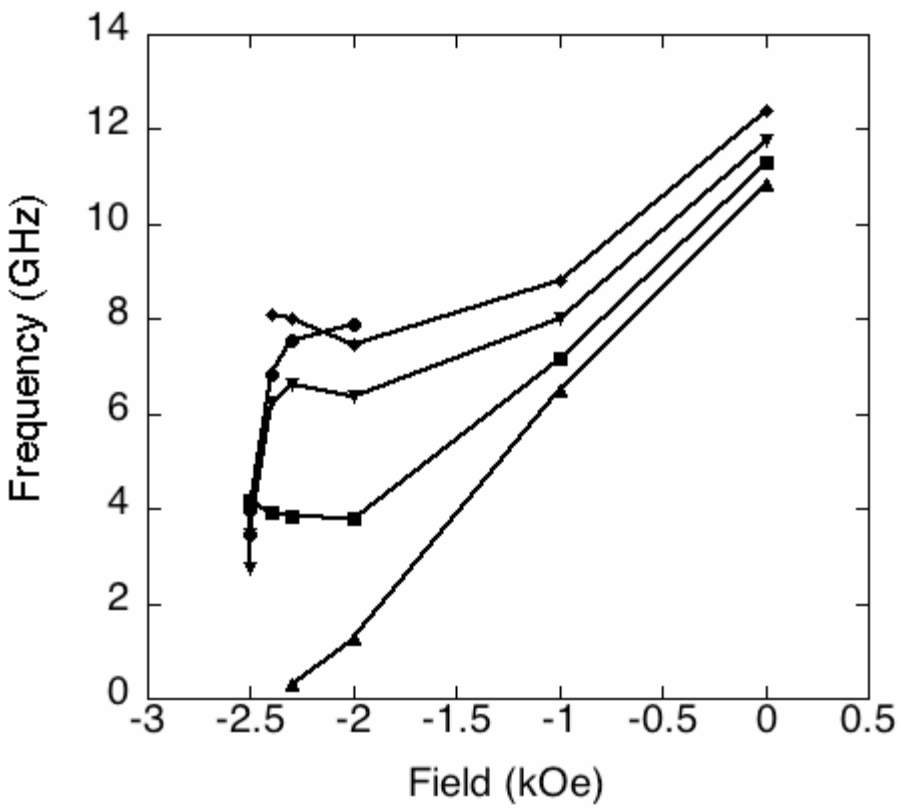

Figure A-1: Frequency versus magnetic field for the lowest frequency modes when a large magnetic field is applied along the anisotropy axis and then reduced and made negative. The equilibrium state is always the centered flower state.

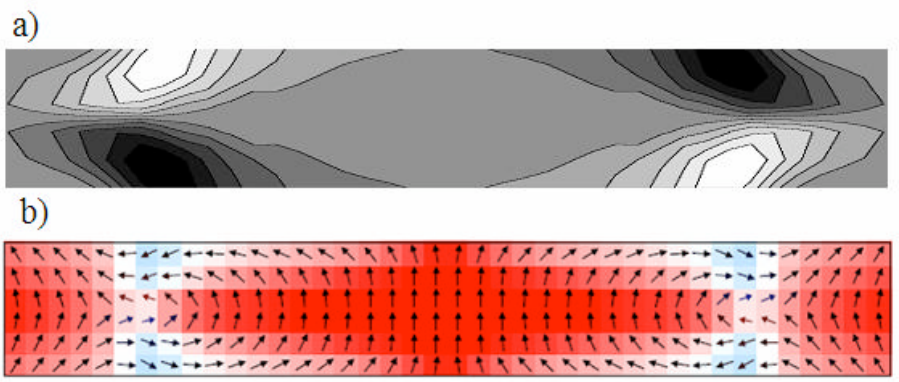

Figure A-2: (a) Out-of-plane component for the 2.731 GHz eigenmode in Fig 8 with the rapid decrease at H_y = -2.503; (b) transient spin configuration found by micromagnetic simulations at H_y = -2.51 kOe.